Correlation Technologies for OTA Testing of mmWave Mobile Devices Using Energy Metrics

S. Wane[1], T.V. Dinh[1], Q.H. Tran [1], D. Bajon[1], F. Ferrero[2], L. Duvillaret[3], G. Gaborit[3,4], J. Sombrin[1],
E. de Lédinghen[5], P. Laban[5], V. Huard[6], S. Mhira[6], L. Tombakdjian[1,2], P. Ratajczak[7], A. Bousseksou[8]

[1]eV-Technologies, France
[2] LEAT-CREMANT, France
[3] Kapteos SAS, France
[4] Université Savoie-Mont-Blanc, France
[5] Synergie-CAD PSC, France
[6]Dolphin-Design, France
[7]ORANGE-Labs, France
[8]LCC-CNRS, France

Abstract—In this paper, we introduce correlation technologies both at RF/mmWave and Base-Band frequencies. At RF and mmWave frequencies power-spectra and energy-spectra metrics are introduced for measuring the power-density of mobile devices and systems. The use of unified power-spectra and energy-spectra metrics leads to innovative *Electromagnetic-Thermal sensing* solutions for OTA-Testing. At Base-Band frequencies, DSP-based Convolutional-Accelerators are proposed for fast and accurate measurement of EVM (Error Vector Magnitude) using correlation technologies. New *ASIC-embedded Smart-Connectors* are developed for bringing correlation-based signal processing close to antenna-in-package (AiP) modules. Porting of the DSP-based Convolutional-Accelerators into advanced FD-SOI-ASIC platforms for co-integration with adaptive RF/mmWave Front-End-Modules will enable real-time extraction of *auto-correlation* and *cross-correlation* functions of stochastic signals for mobile devices and systems. Perspectives toward optically synchronized interferometric-correlation technologies are drawn for accurate measurements of stochastic EM fields in noisy environments.

I. INTRODUCTION

In this contribution, we introduce *Correlation Technologies* both at RF/mmWave and Base-Band frequencies for OTA testing of mobile devices and systems. The originality of the proposed solutions reside in the following attributes:

- *At RF and mmWave frequencies*, energy and power-density based metrics are used for near-field and far-field sensing.
- *At Base-Band frequencies*, new *DSP-based Convolutional-Accelerators* are proposed for pushing EVM measurement solutions to industrial-testing both in connectorized and OTA configurations.
- *ASIC-embedded Smart-Connectors* are proposed for co-design and co-integration of adaptive Front-End-Modules with *Antenna-in-Package* (AiP) modules.

In Fig.1(a), an adaptive front-end-module (AFEM) implementing unified RF/mmWave and Base-Band correlation technologies is presented. The front-end-module provides adjustable 80 dB dynamic range for efficiently characterizing user-equipment (UE) mobile devices using power-density and energy-density metrics. The AFEM is combined with *Mosaic-based* array technologies built using Wafer-Level-Chip-Scale-Packaging (WLCSP) compliant with antenna-in-package (AiP) solutions. The resulting *AFEM-AiP* co-design enables radical

vision: replacing antenna arrays with energy-efficient and affordable '*Smart Integrated Electromagnetic Emitting and Receiving surfaces and volumes*', conformal to the shape of the object they are installed on.
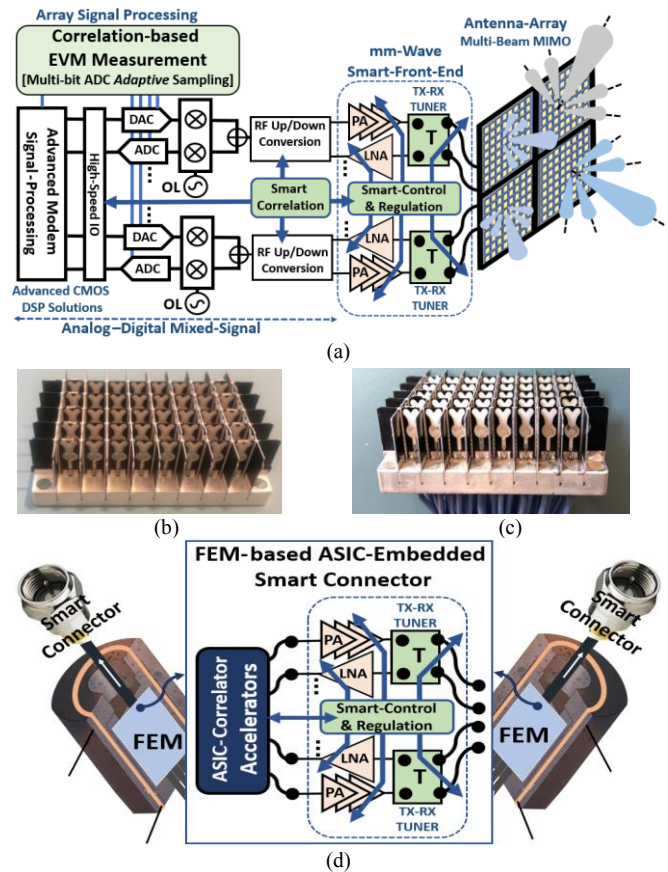

Fig. 1. (a) Wireless adaptive Front-End-Modules including advanced auto and cross-correlation signal processing and Multi-Beam MIMO antennas. 64-Elements Vivaldi-Antenna array for OTA applications without (b) and with (c) cabling. (d) Smart-Connectors with embedded Front-End-Modules.

This approach will drive the next generation of communication and sensing equipments using unified Electromagnetic-Thermal power-density and energy-density metrics. The underlying technological solution consists of eliminating the concept of "elements" in arrays. The radiating

current flows over a textured surface ("*metasurface and metavolumes*") that is fed by a limited number of emitting/receiving points (or "ports"), through which the *AFEM-AiP* system can sense the near-field and far-field *Electromagnetic-Thermal* energy flows and adapt to it. Innovative hybrid *Electromagnetic-Thermal* sensing solution is introduced based on spintronics crossover materials exhibiting functionalized fluorescence. Correlation-based interferometric synchronization of Electromagnetic and Thermal sensing will open new possibilities for OTA industrial testing of MIMO devices and systems accounting for beamforming capabilities. Hybrid *Electromagnetic-Thermal* sensing using the proposed spintronics technologies leads to straightforward extraction of time-varying temperature heatmaps for broadband measurement of *Specific Absorption Rate* (SAR).

II. MAIN RESULTS, ANALYSIS AND DISCUSSION

A. Correlation Technologies for OTA-Testing of Mobile Devices and Systems Using Energy Metrics

Field-Field Correlation Functions (FF-CF), in revealing unified information about the signals to which they refer and the space through which the radiation [1] has propagated, provide solid foundations for bridging modeling and measurement into a consistently complementary framework. In a broad range of applications including ultrasonics [2], underwater acoustics [3], geophysics [4], it is observed that the Green's function can be retrieved by cross-correlating fluctuations recorded at two locations. For structures that are not invariant under time reversal, it is demonstrated [5] that the fluctuations must be excited by volume sources in order to satisfy the energy balance (equipartitioning) that is required to retrieve the Green's function. The extracted cross-correlation [6] can be linked to the general theory of coherence [7], [8]. For deterministic noise power density distribution, the challenge of energy detection of unknown signals in presence of noise is discussed in [9]. For stochastic signals, it is established that numerical values of noise amplitudes cannot be specified. Thus, for modeling and measuring stochastic signals, it is required to deal with energy and power spectra [7-8] through the extraction of correlation functions. The energy density can be written as the sum of electric and magnetic energy densities [1]:

$$W(\rho) = W_E(\rho) + W_H(\rho) \quad (1)$$

$$W_E(\rho) = \frac{\varepsilon}{2}|E(\rho)|^2 \quad and \quad W_H(\rho) = \frac{\mu}{2}|H(\rho)|^2 \quad (2)$$

The correlation function of the electric or magnetic field is defined as:

$$C_X^{FF} \equiv \frac{\langle X(\rho_1).X^*(\rho_2)\rangle}{\langle|X(\rho_1)|^2\rangle\langle|X(\rho_2)|^2\rangle} \quad (3)$$

where $\langle X \rangle$ refers to ensemble average (expectation) applied to stochastic variable X and * stands for complex conjugate.

The correlation function of the electric and magnetic energies density can be deduced as:

$$C_{W_E}^{FF}$$
$$\equiv \frac{\langle[W_E(\rho_1)-\langle W_E(\rho_1)\rangle][W_E(\rho_2)-\langle W_E(\rho_2)\rangle]\rangle}{\sqrt{\langle[W_E(\rho_1)-\langle W_E(\rho_1)\rangle]^2\rangle\langle[W_E(\rho_2)-\langle W_E(\rho_2)\rangle]^2\rangle}} \quad (4)$$

$$C_{W_H}^{FF}$$
$$\equiv \frac{\langle[W_H(\rho_1)-\langle W_H(\rho_1)\rangle][W_H(\rho_2)-\langle W_H(\rho_2)\rangle]\rangle}{\sqrt{\langle[W_H(\rho_1)-\langle W_H(\rho_1)\rangle]^2\rangle\langle[W_H(\rho_2)-\langle W_H(\rho_2)\rangle]^2\rangle}} \quad (5)$$

For stationary stochastic signals, the spatial correlation functions for the total field X_t exhibit a $SinC(k\rho)$ law.

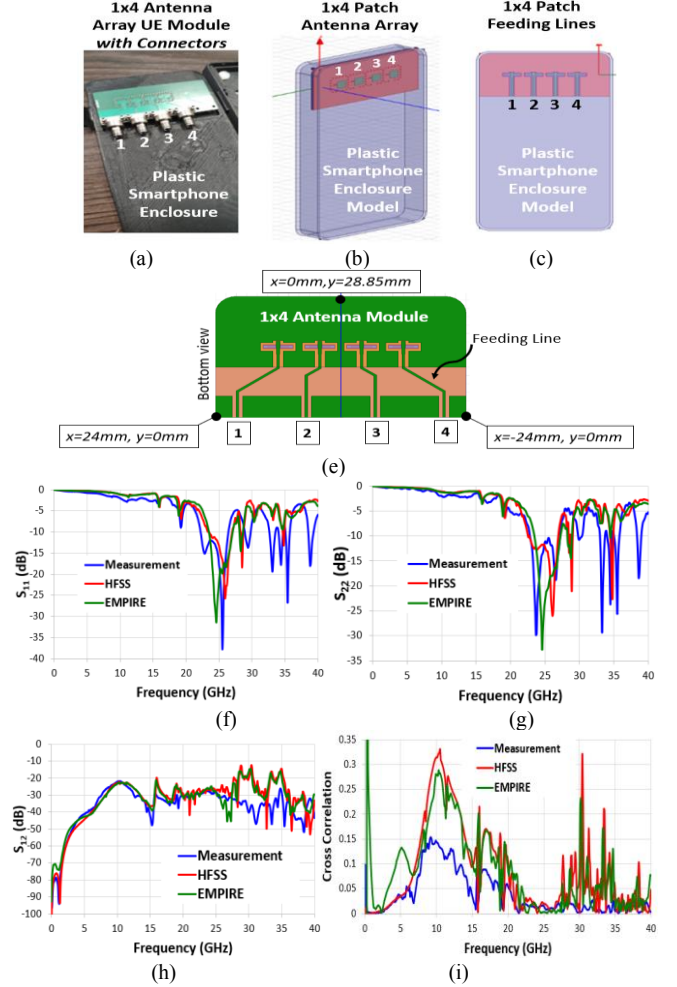$$C_{X_t}^{FF}(\rho) = \propto SinC(k\rho) \quad (6)$$

Fig.2 Experimental 26GHz DUT with connectorized 1x4 antenna array (a) and associated 3D Model including enclosure (b) and feeding lines (c) built using Full-Wave solvers in time and frequency domains. DUT near-field scanning area for power & energy density extractions (d). Broadband measurement of return-losses S_{11}(f), S_{22} (g) and near-coupling S_{12} (h) of the antenna elements compared to 3D Full-Wave simulations. Measured correlation functions (i) versus 3D Full-Wave simulations as function of frequency.

The spatial correlation functions of the transverse components X_t can be expressed as:

$$C_{X_t}^{FF}(\rho) = \frac{3}{2}\left\{SinC(k\rho) - \frac{1}{(k\rho)^2}\left[SinC(k\rho) - \kappa SinC\left(\frac{k\rho}{2}\right)\right]\right\} \quad (7)$$

where it can be established that $\kappa = cos\left(\frac{k\rho}{2}\right)$.

The $SinC(k\rho)$ law can be implemented using advanced signal processing convolutional accelerators implementing broadband expansions:

$$SinC(k\rho) = \frac{Sin(k\rho)}{k\rho} = \sum_{n=1}^{n=\infty}(-1)^n\frac{(k\rho)^{2n}}{(2n+1)!} \quad (8)$$

$$SinC(k\rho) = \prod_{k=1}^{\infty} \cos\left(\frac{k\rho}{2^k}\right) \qquad (9)$$

The proposed analysis is evaluated using 5G NR FR2 antenna array (1×4 elements) module as DUT (Fig.2) for frequencies in the band from 26 GHz to 30 GHz. The unitary antenna element composing the array is based on the aperture-coupled structure introduced in [10]. A 4×4 mm² patch is placed 2mm above the upper slot introducing an additional resonance which allows the single-element bandwidth and gain to be increased. The antenna module is connectorized (see Fig.2(a)-d)) for a 4-Port measurement configuration using both frequency and time-domain instruments with and without down-conversion to sub-6 GHz frequency bands. The single-element S_{22}, $S_{11} \leq -10$ dB impedance bandwidth is from 24.25 to 27.5 GHz as shown in Fig.2 (f-g) comparing measurement and simulations using 3D full-wave solvers (HFSS, EMPIRE and CST).
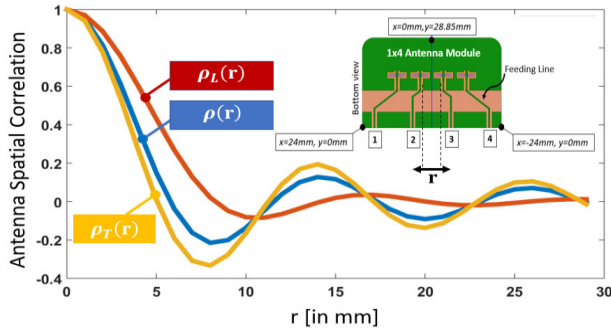

Fig.3: Transverse, Longitudinal and total antenna spatial correlation as a function of the separation distance r between array elements.

In Fig.3, the longitudinal, transverse and total correlation functions are shown as function of the $SinC(k\rho)$ law approximation order. It is observed that only few numbers of terms are required to reach very accurate estimations (*below 1% uncertainties* for near-field OTA sensing).

B. Spintronics-based EM-Thermal Co-Design Toward High-Resolution Near-Field Sensing of Power and Energy Density Metrics

Use of electromagnetic infrared techniques for visualizing and measuring microwave fields is well known [11-12], following the pioneering work of Hasegawa [12] in 1995. The available techniques consist in inserting sensitive films with electric and/or magnetic properties which induce currents resulting in heating recorded by the infrared cameras. However, today, to our best knowledge, available solutions are based on materials that demand for high input powers up to several tens of dBm which lead to low heating effects very difficult to use for OTA-Testing of devices and systems. We propose alternative solutions based on the use of quantum spin-crossover (SCO) materials exhibiting functional properties [13] which are responsive to multi-physics external stimuli such as temperature, pressure, light irradiation, electromagnetic field, radiation, nuclear decay, soft-X-ray, (de)solvation. We introduce new Electromagnetic-Thermal sensing solutions using SCO materials compliant with FDSOI technologies [13] for near-field and far-field characterization of electronic circuits and radiating systems. Use of innovative correlation

technologies [15] is combined with advanced interferometric synchronized sampling for accurate extraction of vectorial power and energy density metrics in time and frequency domains. Fig.4 represents the power-density as function of distance from the DUT. In Fig.6 (a), (b), (c), the Electromagnetic-Thermal sensing reference plane for power and energy density is at 10 mm above the DUT, which is the bottom of the thermal indictor material.
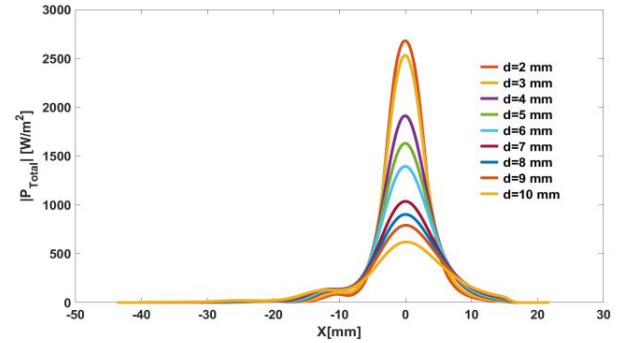

Fig. 4: Extracted power-density as a function of the distance *d* of Probing system to DUT at 26 GHz.

Fig.5 illustrates a synoptic view of the proposed EM-Thermal conversions using both IR-cameras and visible cameras. In Fig.5, two separate functionalizations are considered distinctly for the coating of the SCO material on the DUT side and on the IR/Visible camera side. Such functionalizations can benefit from *metasurface* technologies [14] using 3D inhomogeneous patterning techniques.
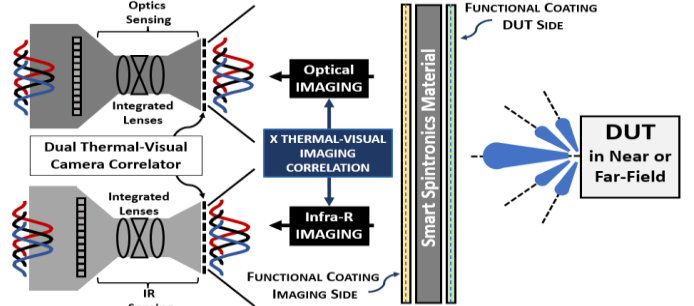

Fig. 5: Smart functionalized spintronics material for Electromagnetic-Thermal sensing in near and far field using Dual IR-Optical Camera.

It is observed that a direct link can be established between the thermal variations on the indicator material and the square of the electric field. Few tens of dBm input power on the radiated element allows obtaining a few degrees heating dynamic on the used thermal indicator from which field amplitudes can be deduced following simple relations:

- *For Electric-Field as primary sensing field:*

$$|E| = X_{EM-Thermal}^{E}\sqrt{\Delta T_{Averaged}} \qquad (10)$$

- *For Magnetic-Field as primary sensing field:*

$$|H| = X_{EM-Thermal}^{H}\sqrt{\Delta T_{Averaged}} \qquad (11)$$

In equations (10) and (11) $X_{EM-Thermal}^{E}$ and $X_{EM-Thermal}^{H}$ are conversion coefficients that depend on the heat transfer coefficient, the heat capacity, the density of the thermal

indicator material and the frequency. From equations (10) and (11) the power density (spatially averaged) appears in the form:

$$|sPD| = \propto X^E_{EM-Thermal} X^H_{EM-Thermal} \Delta T_{Averaged} \qquad (12)$$

In Fig.6 (d) and Fig.6 (e) a setup based on the configuration of Fig.5 is used based on a thermal indicator material with $tan(\delta)=0.022$. The thermal conductivity of the thermal indicator material is *0.2 W/(m.K)* for a convection coefficient of *15.3 W/(m².K)* and a relative radiation coefficient equal to *1*. The EM-Thermal co-design model is meshed using *5.3 Mcells (334×52×104)*.

(a)   (b)

(c)

(d)   (e)
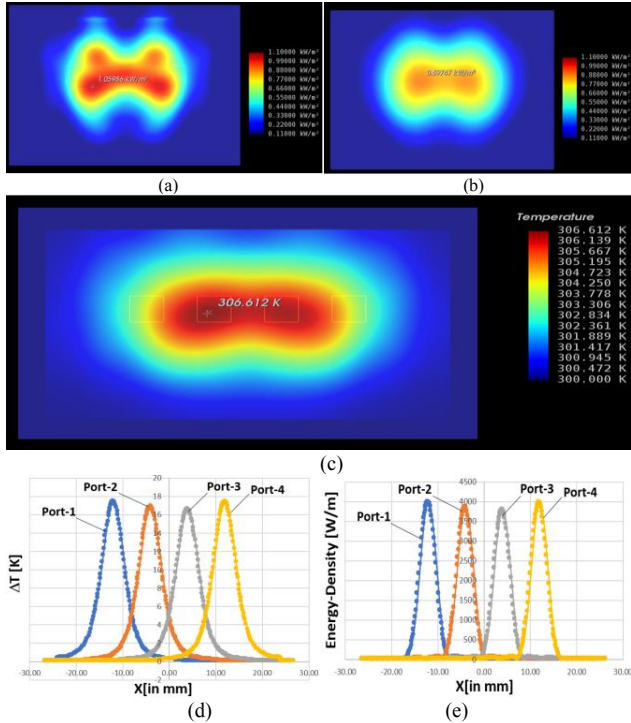
Fig.6: Extracted power density (a) and averaged power-density (b) at 26 GHz based on simultaneous excitation 0° phase offset. Extracted thermal distribution (c) on the thermal indicator material at 26 GHz. Extracted thermal distribution for sequential excitations of the four ports of the DUT at 26 GHz (d). Energy density (e) for sequential excitations of the four ports of the DUT at 26 GHz.

III. Conclusion

In this paper, we have presented correlation technologies for measuring power-density and energy-density of mobile devices and systems. New *ASIC-embedded Smart-Connectors* are developed for bringing correlation-based signal processing close to antenna modules. The use of unified power-spectra and energy-spectra metrics leads to innovative *Electromagnetic-Thermal sensing* solutions for OTA measurement of RF and mmWave devices using quantum spin-crossover materials combined with both IR and Visible imagers. The imaging solutions have been applied to mmWave beamforming modules demonstrating the possibility of extracting *power-density* and *energy-density* metrics *as function of beamsteering angles*. Porting of Spintronics hybrid Thermal-Electromagnetic imaging into advanced FD-SOI platforms is proposed. The co-integration of SCO materials with smart FEMs will foster new possibilities for replacing conventional IR-imagers by low-cost visible imagers with fluorescent functionalization processes. At

Base-Band frequencies, ongoing work is relative to new DSP-based *Convolutional-Accelerators* compliant with IEEE P1765 standard for pushing EVM measurement solutions [16] to industrial testing both in connectorized and OTA configurations using *Correlation Technologies*. Implementation of DSP-based Convolutional Accelerators into advanced FD-SOI-ASIC platforms for co-integration with adaptive RF/mmWave Front-End-Modules will enable real-time extraction of *auto-correlation* and *cross-correlation* functions of stochastic signals for mobile devices and systems.

References

[1] R. F. Harrington, Time-Harmonic Electromagnetic Fields. New York: McGraw-Hill, 196.

[2] R. L. Weaver and O. J. Lobkis, ''Ultrasonics without a source: Thermal fluctuation correlations at MHz frequencies,'' Phys. Rev. Lett. 87, 134301-2001.

[3] P. Roux and W. A. Kuperman. "Extracting coherent wavefronts from acoustic ambient noise in the ocean". The Journal of the Acoustical Society of America, 116(4):1995–2003, Oct 2004.

[4] J. Rickett, & J. F. Claerbout, "Acoustic daylight imaging via spectral factorization; helioseismology and reservoir monitoring", The Leading Edge, 18(8), 957–960,1999.

[5] R. Snieder, et al., "Unified Green's function retrieval by cross-correlation; connection with energy principles". Physical Review. E, Statistical, Nonlinear, and Soft Matter Physics. 75: 036103. PMID 17500755.

[6] S. Wane, R. Patton, and N. Gross, "Unification of instrumentation and EDA tooling platforms for enabling smart chip-package-PCB-probe arrays co-design solutions using advanced RFIC technologies," in IEEE Conf. on Ant. Measurements Applications, Sept 2018, pp. 1–4.

[7] B. Fourestie, J.-C. Bolomey, et al., "Spherical Near Field Facility for Characterizing Random Emissions", IEEE Trans. On Ant. and Prop., Vol. 53, no. 8, pp. 2582-2588, August 2005.

[8] E. Wolf, "New theory of partial coherence in the space–frequency domain. Part I: spectra and cross spectra of steady-state sources", J. Opt. Soc. Am. 72, 343–351 (1982).

[9] H. Urkowitz, "Energy detection of unknown deterministic signals," Proc. IEEE, vol. 55, no. 4, pp. 523–531, 1967.

[10] Nguyen, T.Q.K., et al., "Experimental evaluation of user's finger effects on a 5G terminal antenna array at 26 GHz". IEEE Antennas Wirel. Propag. Lett., 1–1 (2020).

[11] D. Prost, F. Issac, F. Lemaitre, J.P. Parmantier "Infrared Thermography of Microwave Electromagnetic Fields", D, EMC Europe, Rome, (2012).

[12] H. Ragazzo, et al., "Detection and imaging of magnetic field in the microwave regime with a combination of magnetic losses material and thermo-fluorescent molecules," IEEE Trans. Magn., vol. 55, no. 2, pp. 1–4, Feb. 2019, doi: 10.1109/TMAG.2018.2860520.

[13] S. Wane, Q.H. Tran, et al., "Smart Sensing of Vital-Signs: Co-Design of Tunable Quantum-Spin Crossover Materials with Secure Photonics and RF Front-End-Module", IEEE-MTT-Texas symposium 2021.

[14] M. Bodehou, E. Martini, S. Maci, I. Huynen and C. Craeye, "Multibeam and beam scanning with modulated metasurfaces," IEEE Trans. Antennas Propag., vol. 68, no. 3, pp. 1273-1281, Mar. 2020.

[15] S. Wane, et al., "Correlation Technologies for OTA Testing of Mobile Devices: Power-Density Measurement", in IEEE Conf. on Ant. Measurements Applications, Nov. 2021.

[16] J. Sombrin, "On the formal identity of EVM and NPR measurement methods: Conditions for identity of error vector magnitude and noise power ratio," in EuMC Proc., Manchester, UK, 2011, pp. 337–340.